

Electronic Supplementary Information

Paraffinic metal-organic polyhedral cages: Solution-processable porous modules exhibiting three-dimensional molecular order

1. Abbreviations	page S2
2. Materials and methods	page S2
3. Preparation of paraffinic ligands H₂L	page S3
4. Metal complexation reactions of paraffinic ligands H₂L	page S8
5. X-ray diffraction analysis of organized structure of MOP	page S11
6. Thermal analysis and discussion	page S14
7. References	page S16

1. Abbreviations

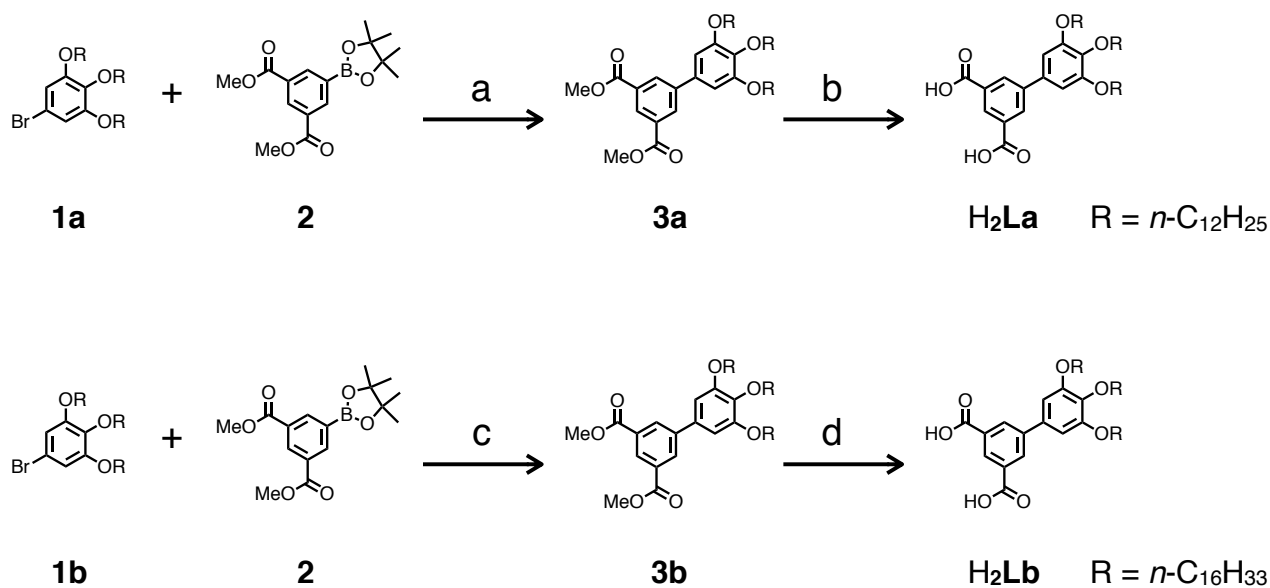
EtOAc: ethylacetate, APCI-TOF: atmospheric pressure chemical ionization time-of-flight, DCTB: *trans*-2-[3-(4-*tert*-butylphenyl)-2-methyl-2-propenylidene]malononitrile, DEF: *N,N*-diethylformamide, DMSO: dimethylsulfoxide, DMA: *N,N*-dimethylformamide, dppf: 1,1'-bis(diphenylphosphino)ferrocene, HPLC: high performance liquid chromatography, MALDI-TOF: Matrix-assisted laser desorption ionization time-of-flight, NMR: nuclear magnetic resonance, OAc: CH₃COO, SAXS: small angle X-ray scattering, SEC: size exclusion chromatography, THF: tetrahydrofuran, TMS: tetramethylsilane, UV: ultraviolet, XRD: X-ray diffraction.

2. Materials and methods

All solvents, organic and inorganic reagents are commercially available, and were used without further purification. 5-Bromo-1,2,3-tris(dodecyloxy)benzene (**1a**), 5-bromo-1,2,3-tris(hexadecyloxy)benzene (**1b**), and dimethyl-5-(4,4,5,5-tetramethyl-1,3,2-dioxaborolan-2-yl)isophthalate (**2**) were synthesized according to previously reported procedures.¹ Single crystals of Cu₂₄Ip/Bu₂₄ (Ip/Bu²⁻: 5-*tert*-butylisophthalate) were prepared according to previously reported procedures.² Silica-gel column chromatography was performed using Wakogel silica gel C-200 (64–210 μm). NMR spectroscopic measurements were performed using JEOL model ECS-400 (400 MHz for ¹H, 100 MHz for ¹³C) spectrometer. NMR spectra were calibrated as below; *d*₆-DMSO: CHD₂CD₃SO = 2.50 ppm for ¹H, (CD₃)₂SO = 39.52 ppm for ¹³C; CDCl₃: (CH₃)₄Si = 0.00 ppm for ¹H, (CH₃)₄Si = 0.00 ppm for ¹³C. APCI-TOF mass spectra were recorded on a Bruker model micrOTOF II. MALDI-TOF mass spectra were recorded on a Bruker model Ultraflex III using DCTB as a matrix. Analytical SEC was performed at 313 K on a Shimadzu model HPLC Prominence system with two polystyrene gel columns in series (Shodex KF-804L) equipped with a refractive index detector (Shimadzu RID-10A) and an UV detector (Shimadzu SPD-20A). The mobile phase was THF at a flow rate of 1.0 mL/min. XRD analyses were carried out using a Rigaku SmartLab diffractometer (CuKα) equipped with a temperature-controlled sample stage and Dectoris model PILATUS 200 K detector. Synchrotron radiation (SR) XRD data for the structural analysis of **MOP-a_{DMA}** were collected using a synchrotron X-ray beam (λ = 0.92 Å) of BL8S3 beam line at AichiSR, Japan, equipped with a temperature controller (Linkam Scientific Instrument) and R-Axis IV++ detector. Variable-temperature SR-XRD data were also collected using a synchrotron X-ray beam (λ = 1.0 Å) of BL45XU at SPring-8, Japan, equipped with a customized Linkam Scientific Instrument temperature controller and Dectoris model PILATUS 3X 2M detector. Thermogravimetric analyses (TGA) were carried out using Rigaku model Thermo plus EVO. Differential scanning calorimetry (DSC) was carried out using Hitachi High-Tech Science Corp. model DSC7020 at the scanning rate of 10 °C/min.

3. Preparation of paraffinic ligands H₂L

Scheme S1. Synthetic routes for paraffinic ligands H₂L.



Reagents and conditions: (a) Pd(dppf)Cl₂, Na₂CO₃aq., THF, 80 °C, 16 h, (86%); (b) (i) KOH_{aq.}, THF, reflux, 16 h, (ii) HCl_{aq.}, 0 °C, (quant.); (c) Pd(PPh₃)₄, Na₂CO₃aq., THF, 80 °C, 16 h, (59%); (d) (i) KOH_{aq.}, THF, reflux, 16 h, (ii) HCl_{aq.}, 0 °C, (95%).

Dimethyl-3',4',5'-tris(dodecyloxy)-[1,1'-biphenyl]-3,5-dicarboxylate (**3a**)

5-Bromo-1,2,3-tris(dodecyloxy)benzene (**1a**) (2.00 g, 2.82 mmol, 1.0 eq), dimethyl-5-(4,4,5,5-tetramethyl-1,3,2-dioxaborolan-2-yl)isophthalate (**2**) (1.17 g, 3.67 mmol, 1.3 eq), 2 M Na₂CO₃aq. (14.1 mL, 28.2 mmol, 10.0 eq), Pd(dppf)Cl₂ (103 mg, 0.14 mmol, 0.05 eq), and THF (28 mL) were placed in a flask. The inner gas was replaced with N₂, and the mixture was stirred at 80 °C for 16 h. After cooling down to room temperature, the reaction mixture was filtered through celite, and the filtrate was extracted with EtOAc. The organic phase was washed with brine, dried over Na₂SO₄, and evaporated under reduced pressure to obtain a black solid. The crude product was purified by column chromatography (SiO₂, EtOAc/*n*-hexane = 5/95) to afford **3a** (2.00 g, 2.43 mmol, 86%) as a pale yellow solid.

¹H NMR (400 MHz, CDCl₃, 298 K, Fig. S1): δ (ppm) = 8.62 (t, *J* = 1.4 Hz, 1H, Ar-*H*), 8.39 (d, *J* = 1.4 Hz, 2H, Ar-*H*), 6.79 (s, 2H, Ar-*H*), 4.05 (t, 4H, *J* = 6.7 Hz, CH₂), 4.00 (t, *J* = 6.7 Hz, 2H, CH₂), 3.98 (s, 6H, CH₃), 1.71–1.89 (m, 6H, CH₂), 1.44–1.54 (m, 6H, CH₂), 1.20–1.40 (m, 48H, CH₂), 0.88 (t, *J* = 6.7 Hz, 9H, CH₃).

¹³C NMR (100 MHz, CDCl₃, 298 K, Fig. S2): δ (ppm) = 166.3, 153.6, 142.3, 138.7, 134.4, 132.2, 131.0, 129.0, 106.1, 73.6, 69.5, 52.5, 32.0, 30.4, 29.8–29.3, 26.2, 26.1, 22.7, 14.1. (The signals of alkyl side chains are overlapped.)

APCI-TOF mass (positive): calcd. for [C₅₂H₈₆O₇ + H]⁺, *m/z* = 823.64; found *m/z* = 823.66.

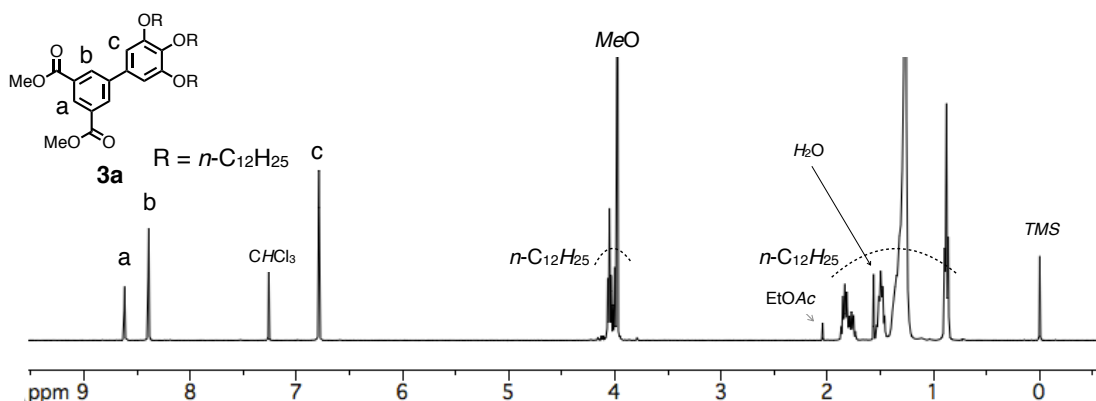


Figure S1. ¹H NMR spectrum of **3a** (400 MHz, CDCl₃, 298 K).

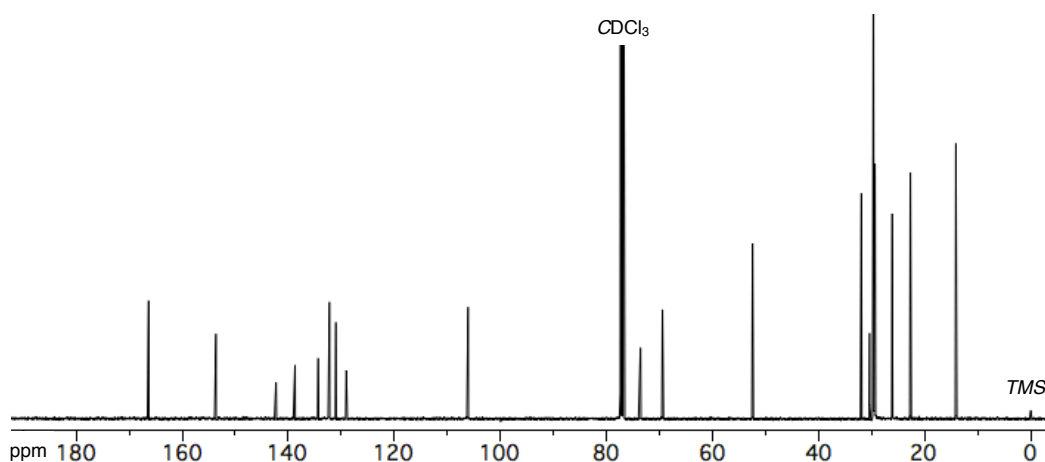


Figure S2. ¹³C NMR spectrum of **3a** (100 MHz, CDCl₃, 298 K).

3',4',5'-Tris(dodecyloxy)-[1,1'-biphenyl]-3,5-dicarboxylic acid (**H₂La**)

To the mixture of **3a** (2.55 g, 3.10 mmol) and THF (26 mL) was added 2 M KOH aq. (15.5 mL, 31.0 mmol), which was then refluxed for 16 h. After cooling down to 0 °C, the reaction mixture was acidified with conc. HCl aq.. The resulting precipitate was collected by filtration, washed with water, and dried under reduced pressure at 60 °C for 2 days to afford **H₂La** (2.47 g, 3.10 mmol, quant.) as a colorless solid.

¹H NMR (400 MHz, *d*₆-DMSO, 373 K, Fig. S3): δ (ppm) = 13.3–12.4 (br, 2H, COOH), 8.44 (br, 1H, Ar-H), 8.30 (br, 2H, Ar-H), 6.89 (s, 2H, Ar-H), 4.07 (t, *J* = 6.4 Hz, 4H, CH₂), 3.94 (t, *J* = 6.4 Hz, 2H, CH₂), 1.79–1.64 (m, 6H, CH₂), 1.52–1.41 (m, 6H, CH₂), 1.39–1.20 (m, 48H, CH₂), 0.85 (t, *J* = 6.4 Hz, 9H, CH₃).

¹³C NMR (100 MHz, *d*₆-DMSO, 373 K, Fig. S4): δ (ppm) = 166.0, 152.8, 140.9, 138.2, 133.5, 131.7, 130.6, 128.0, 106.0, 72.2, 30.7, 29.4, 28.6–28.0, 25.1, 21.4, 13.1. (The signals of alkyl side chains are overlapped.)

APCI-TOF mass (negative): calcd. for [C₅₀H₈₂O₇ – H][–], *m/z* = 795.61; found *m/z* = 795.64.

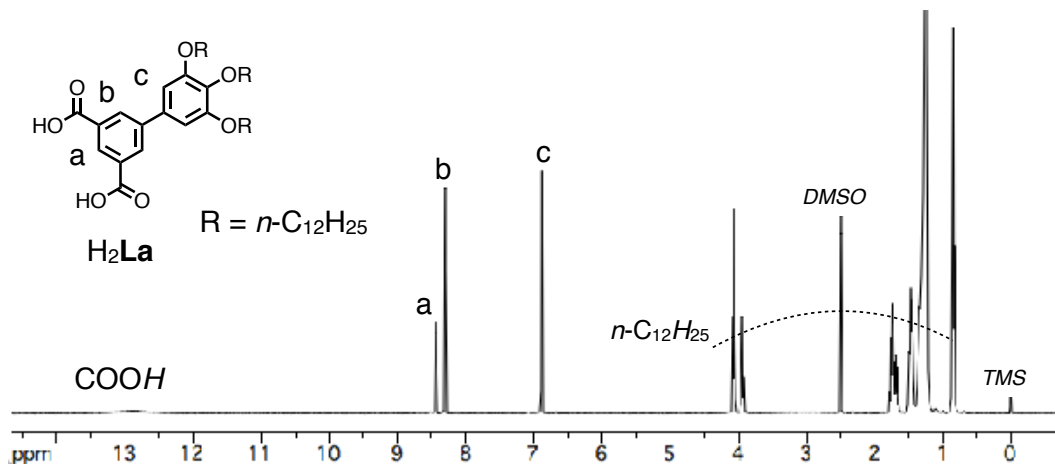


Figure S3. ¹H NMR spectrum of **H₂La** (400 MHz, *d*₆-DMSO, 373 K).

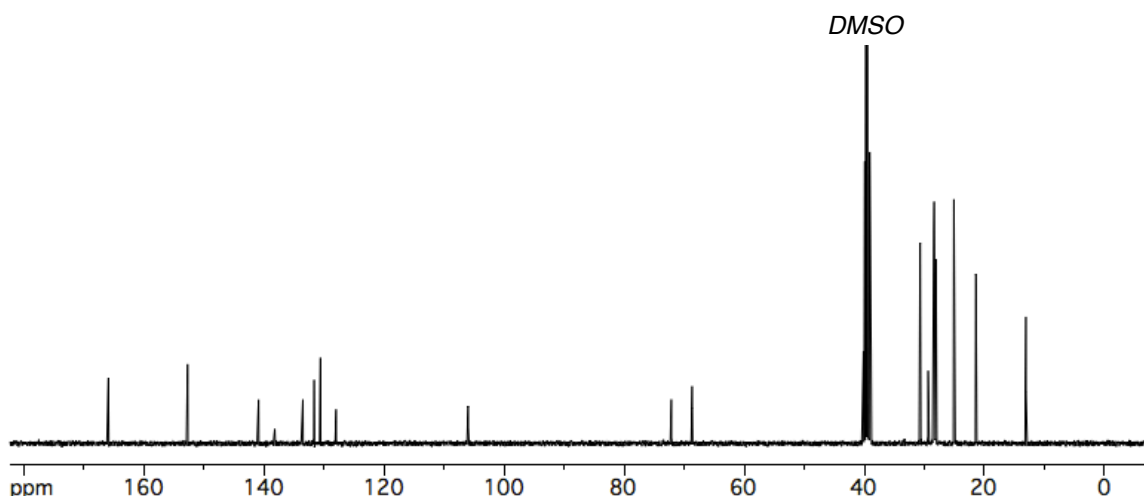


Figure S4. ¹³C NMR spectrum of **H₂La** (100 MHz, *d*₆-DMSO, 373 K).

Dimethyl-3',4',5'-tris(hexadecyloxy)-[1,1'-biphenyl]-3,5-dicarboxylate (**3b**)

5-Bromo-1,2,3-tris(hexadecyloxy)benzene (**1b**) (3.00 g, 3.42 mmol, 1.0 eq), dimethyl-5-(4,4,5,5-tetramethyl-1,3,2-dioxaborolan-2-yl)isophthalate (**2**) (976 mg, 4.10 mmol, 1.2 eq), 2 M Na₂CO₃aq. (17.1 mL, 34.2 mmol, 10.0 eq), Pd(PPh₃)₄ (198 mg, 0.17 mmol, 0.05 eq), and THF (40 mL) were placed in a flask. The inner gas was replaced with N₂, and the mixture was stirred at 80 °C for 16 h. After cooling down to room temperature, the reaction mixture was filtered through celite, and the filtrate was extracted with EtOAc. The organic phase was washed with brine, dried over Na₂SO₄, and evaporated under reduced pressure to obtain a black solid. The crude product was purified by column chromatography (SiO₂, EtOAc/*n*-hexane = 1/30) to afford **3b** (2.00 g, 2.02 mmol, 59%) as a colorless solid.

¹H NMR (400 MHz, CDCl₃, 298 K, Fig. S5): δ (ppm) = 8.62 (t, *J* = 1.4 Hz, 1H, Ar-*H*), 8.39 (d, *J* = 1.4 Hz, 2H, Ar-*H*), 6.79 (s, 2H, Ar-*H*), 4.05 (t, *J* = 6.7 Hz, 4H, CH₂), 4.00 (t, *J* = 6.7 Hz, 2H, CH₂), 3.98 (s, 6H, CH₃), 1.71–1.89 (m, 6H, CH₂), 1.44–1.54 (m, 6H, CH₂), 1.20–1.40 (m, 72H, CH₂), 0.88 (t, *J* = 6.7 Hz, 9H, CH₃).

¹³C NMR (100 MHz, CDCl₃, 298 K, Fig. S6): δ (ppm) = 166.3, 153.6, 142.3, 138.7, 134.4, 132.2, 131.0, 129.0, 106.1, 73.6, 69.5, 52.5, 32.0, 30.4, 29.8–29.3, 26.2, 26.1, 22.7, 14.1. (The signals of alkyl side chains are overlapped.)

APCI-TOF mass (positive): calcd. for [C₆₄H₁₁₀O₇ + H]⁺, *m/z* = 991.83; found *m/z* = 991.84.

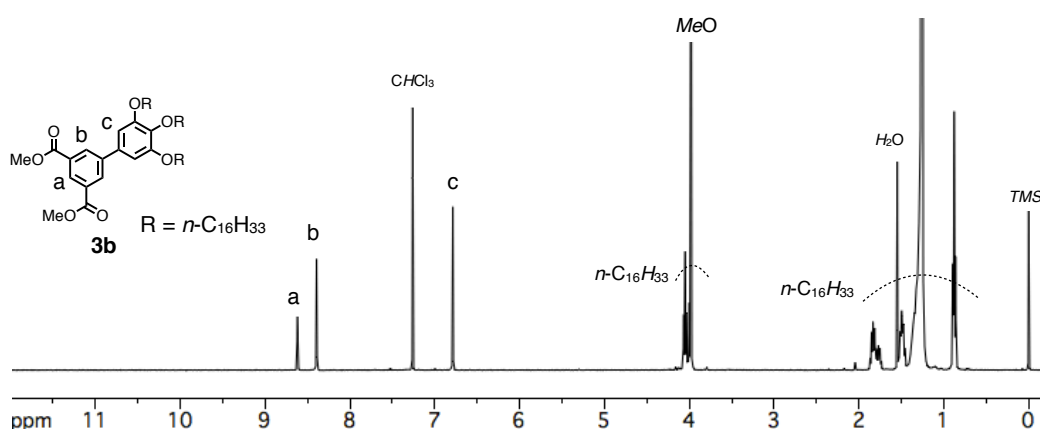


Figure S5. ¹H NMR spectrum of **3b** (400 MHz, CDCl₃, 298 K).

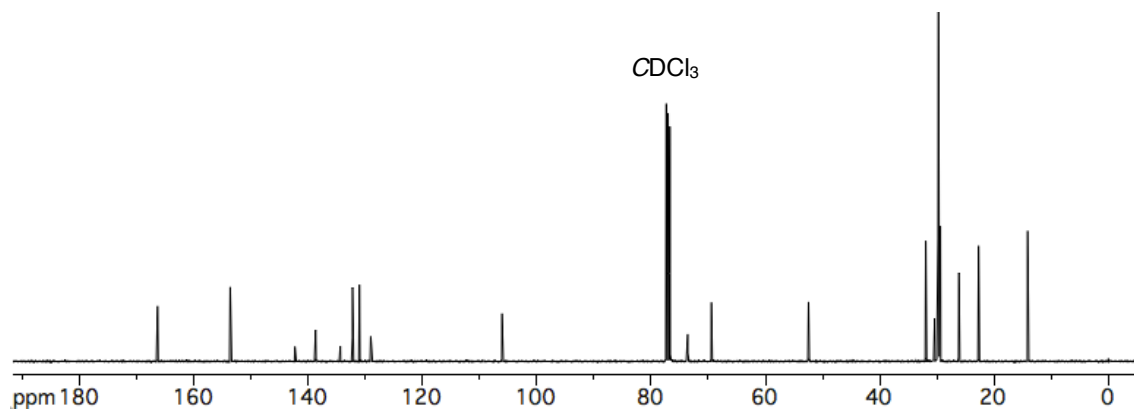


Figure S6. ¹³C NMR spectrum of **3b** (100 MHz, *d*₆-DMSO, 298 K).

3',4',5'-Tris(hexadecyloxy)-[1,1'-biphenyl]-3,5-dicarboxylic acid (**H₂Lb**)

To the mixture of **3b** (1.89 g, 1.91 mmol) and THF (19 mL) was added 2 M KOH aq. (9.6 mL, 19.1 mmol), which was then refluxed for 16 h. After cooling down to 0 °C, the reaction mixture was acidified with conc. HCl aq.. The resulting precipitate was collected by filtration, washed with water, and dried under reduced pressure at 60 °C for 2 days to afford **H₂Lb** (1.74 g, 1.82 mmol, 95%) as a white solid.

¹H NMR (400 MHz, *d*₆-DMSO, 373 K, Fig. S7): δ (ppm) = 13.5–12.4 (br, 2H, COOH), 8.42 (br, *J* = 1.6 Hz, 1H, Ar-*H*), 8.28 (br, *J* = 1.6 Hz, 2H, Ar-*H*), 6.86 (s, 2H, Ar-*H*), 4.04 (t, 4H, *J* = 6.4 Hz, CH₂), 3.91 (br, *J* = 6.4 Hz, 2H, CH₂), 1.78–1.63 (m, 6H, CH₂), 1.53–1.39 (m, 6H, CH₂), 1.39–1.17 (m, 72H, CH₂), 0.84 (br, t, *J* = 6.4 Hz, 9H, CH₃).

¹³C NMR (100 MHz, *d*₆-DMSO, 373 K, Fig. S8): δ (ppm) = 166.0, 152.8, 140.9, 138.2, 133.5, 131.7, 130.6, 128.0, 106.0, 72.2, 30.7, 29.4, 28.6–28.0, 25.1, 21.4, 13.1. (The signals of alkyl side chains are overlapped.)

APCI-TOF mass (negative): calcd. for [C₆₂H₁₀₆O₇ – H][–], *m/z* = 961.79 ; found *m/z* = 961.78.

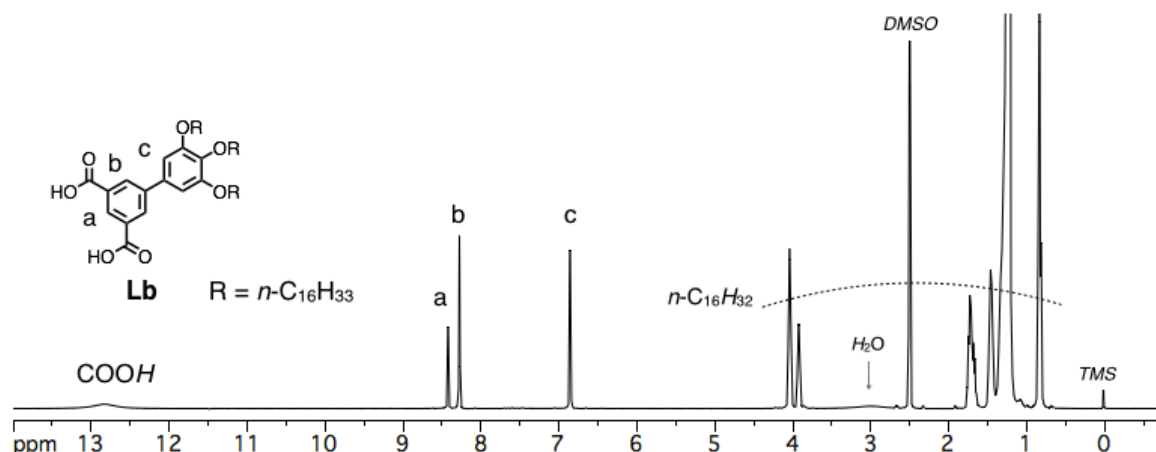


Figure S7. ¹H NMR spectrum of **H₂Lb** (400 MHz, *d*₆-DMSO, 373 K).

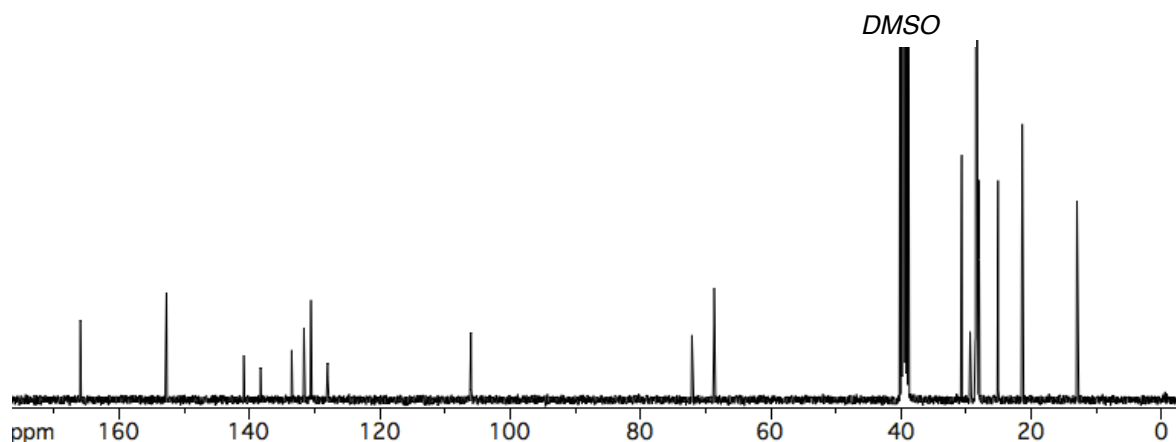


Figure S8. ¹³C NMR spectrum of **H₂Lb** (100 MHz, *d*₆-DMSO, 373 K).

4. Metal complexation reactions of paraffinic ligands H₂L

4-1. Complexation reaction of H₂La and Cu(OAc)₂·H₂O

To a THF solution of H₂La (65 mM, 2.0 mL, 130 μmol, 1.0 eq) was added another THF solution of Cu(OAc)₂·H₂O (33 mM, 5.0 mL, 170 μmol, 1.3 eq). A small aliquot of the resulting mixture was collected and diluted with THF, which was subjected to SEC analysis (Fig. S9b). In order to isolate the product, the reaction mixture was poured into MeOH (25 mL). The product thus precipitated out was purified through reprecipitation method using a mixture of THF (2 mL)/MeOH (20 mL) as a poor solvent for three times, then dried under vacuum at room temperature to afford **MOP-a** (107.2 mg, 5.2 μmol, 96%) as a blue viscous material. The SEC trace and MALDI-TOF mass spectrum, and XRD profile of isolated **MOP-a** are shown in Fig. S9c, Fig. 3 (main text), and Fig. S12a, respectively.

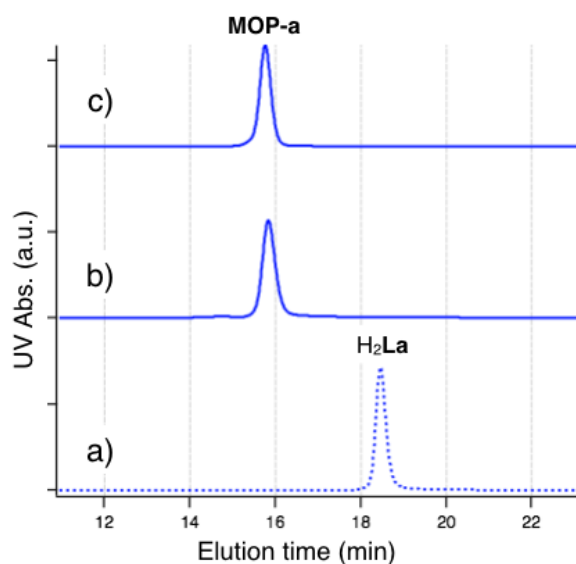


Figure S9. SEC traces of a) H₂La, b) a 1:1.3 mixture of H₂La and Cu(OAc)₂·H₂O in THF, and c) isolated **MOP-a**. SEC charts are recorded at 313 K with a UV detector using THF as the eluent.

4-2. Complexation reaction of H₂Lb and Cu(OAc)₂·H₂O

H₂Lb (408.0 mg, 423 μmol, 1.0 eq) and Cu(OAc)₂·H₂O (90.36 mg, 453 μmol, 1.1 eq) were dissolved in THF (17.5 mL), then the mixture was subjected to sonication at room temperature. A small aliquot of the resulting mixture was collected and diluted with THF, which was subjected to SEC analysis (Fig. S10b). In order to isolate the product, the reaction mixture was poured into MeOH (20 mL). The product thus precipitated out was purified through reprecipitation method using THF and MeOH as a poor solvent for three times, successively washed with MeOH, and then dried under vacuum at room temperature to afford **MOP-b** (397.7 mg, 16.1 μmol, 91%) as a blue viscous material. The SEC trace, MALDI-TOF mass spectrum, and XRD profile of isolated **MOP-b** are shown in Fig. S10c, Fig. S11, and Fig. S12b, respectively.

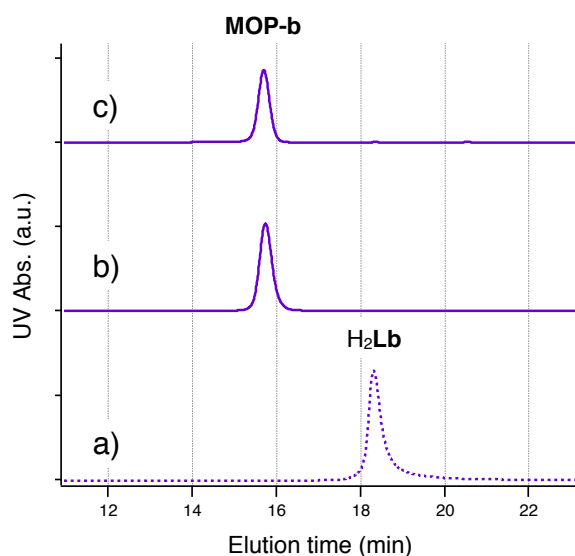


Figure S10. SEC traces of a) H₂Lb, b) a 1:1.1 mixture of H₂Lb and Cu(OAc)₂·H₂O in THF, and c) isolated **MOP-b**. SEC charts are recorded at 313 K with a UV detector using THF as the eluent.

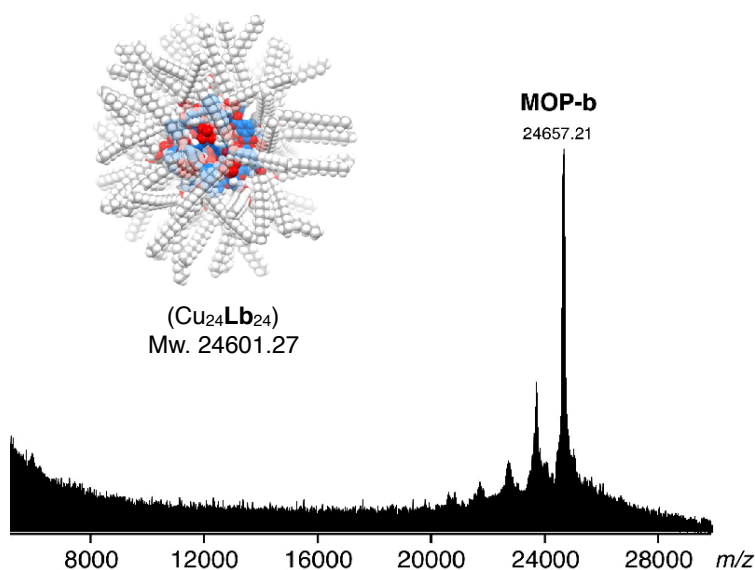


Figure S11. MALDI TOF-mass spectrum (negative) of isolated **MOP-b** (matrix: DCTB).

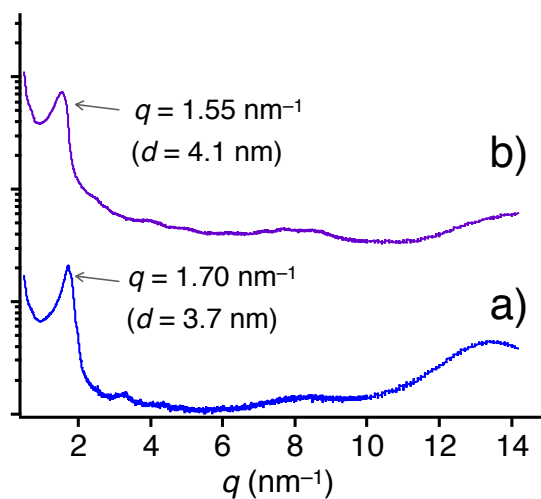


Figure S12. XRD profiles of isolated samples of a) **MOP-a** and b) **MOP-b** (r.t., $\text{CuK}\alpha$, $\lambda = 1.541 \text{ \AA}$).

The XRD profiles of the as-synthesized samples of **MOP-a** and **MOP-b** showed respective single broad peaks around $q = 1.70$ and 1.55 nm^{-1} at room temperature, corresponding to d -spacings of 3.7 and 4.1 nm , respectively (Fig. S12). The observed d -spacing could correspond to the interdistances of the MOP core and depend on the length of the alkyl side chains. The peak broadening observed herein indicates the random arrangement of MOP cores in the dried bulk condition.^{2b}

5. X-ray diffraction analysis of organized structure of MOP

5-1. Preparation of MOP-a_{DMA}

MOP-a (5.35 mg, 0.26 μmol) was placed in a microtube, which was annealed at 80 $^{\circ}\text{C}$ for about 10 min in the presence of DMA (6.5 μL) to obtain **MOP-a_{DMA}** as a blue viscous material. XRD profiles of **MOP-a_{DMA}** are shown in Fig. S13. The content of DMA dopant was calculated to be ca. 60 wt.%.

5-2. Preparation of MOP-b_{DMA}

MOP-b (2.88 mg, 0.12 μmol) was placed in a microtube, which was annealed at 80 $^{\circ}\text{C}$ for about 10 min in the presence of DMA (3.0 μL) to obtain **MOP-b_{DMA}** as a blue viscous material. XRD profiles of **MOP-b_{DMA}** are shown in Fig. S13. The content of DMA dopant was calculated to be ca. 50 wt.%.

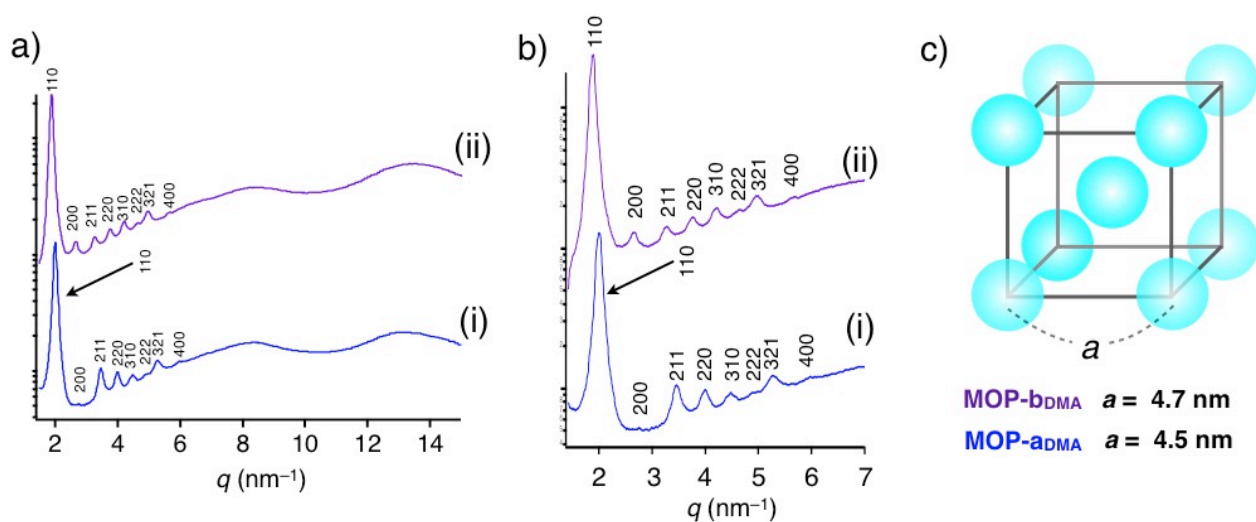


Figure S13. XRD profiles of (i) **MOP-a_{DMA}** and (ii) **MOP-b_{DMA}**; a) whole profiles and b) magnified profiles, and c) their postulated body-centered cubic packing (r.t., $\text{CuK}\alpha$, $\lambda = 1.541$ \AA).

5-3. Synchrotron radiation XRD measurement of MOP-a_{DMA}

MOP-a (4.87 mg, 0.24 μmol) was placed in a borosilicate capillary (diameter: 1.5 mm), which was annealed at 80 $^{\circ}\text{C}$ for about 10 min in the presence of DMA (4 μL) to obtain **MOP-a_{DMA}** as a blue viscous material. The content of DMA dopant was calculated to be ca. 50 wt.%.

Synchrotron radiation (SR) XRD profile of resulting **MOP-a_{DMA}** is given in Fig. S14a that shows many sharp diffraction peaks indexed into a bcc structure (Fig. S13c). Notably, upon removal of DMA from **MOP-a_{DMA}** by heating at 413 K for a few minutes, the structure reorganized into an uncharacterized crystalline structure (Fig. S14b).

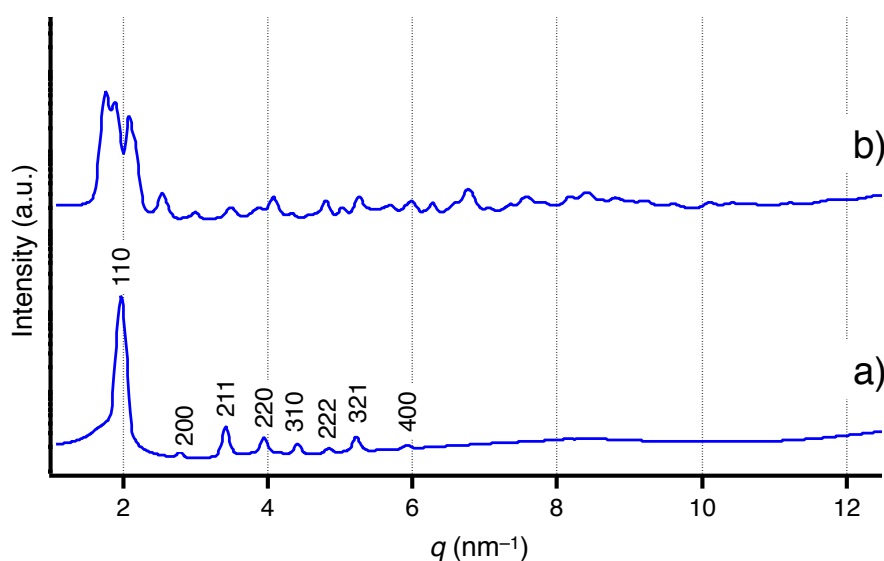


Figure S14. SR-XRD profiles of a) **MOP-a_{DMA}**, and b) **MOP-a_{DMA}** after removing DMA by heating at 413 K measured using synchrotron X-ray beam (313 K, $\lambda = 0.92 \text{ \AA}$) of AichiSR facility, Japan.

Table S1. Summary of experimental and theoretical Millar index of **MOP-a_{DMA}** and **MOP-b_{DMA}**.

		Miller index								$2\sigma^d$		
		110	200	211	220	310	222	321	400			
MOP-a_{DMA}	q (nm ⁻¹)	Experimental ^a	1.89	2.66	3.27	3.75	4.20	4.64	4.96	5.35	0.04	
		Theoretical ^c	1.89	2.67	3.27	3.78	4.23	4.63	5.00	5.35		
	q (nm ⁻¹)	Experimental ^b	1.97	2.80	3.42	3.95	4.41	4.85	5.22	5.93		0.2
		Theoretical ^c	1.97	2.79	3.41	3.94	4.41	4.83	5.21	5.57		

^a Measured at room temperature using CuK α X-ray beam ($\lambda = 1.541 \text{ \AA}$, Fig. S13a-ii).

^b Measured at 313 K using a synchrotron X-ray beam on the BL8S3 beam line at AichiSR ($\lambda = 0.92 \text{ \AA}$, Fig. S14a).

^c Calculated based on lattice constant as follow. **MOP-a_{DMA}**; $a = 4.5 \text{ nm}$, **MOP-b_{DMA}**; $a = 4.7 \text{ nm}$ (Figure S13c).

$$\sigma = \left(\frac{1}{n} \sum (q_{\text{theoretical}} - q_{\text{experimental}})^2 \right)^{1/2}$$

5-4. Film preparation

MOP-b (10.5 mg) was dissolved in *n*-hexane (500 μ L) to give a clear blue solution. The resulting solution was slowly layered on DMA. After slow evaporation of the *n*-hexane layer at room temperature for 4 h, a blue colored self-supporting film was obtained at the interface. The resulted film was robust enough to be collected by tweezers. XRD profiles of the resulting film (Fig. S15b-ii) showed identical diffraction patterns to the bulk **MOP-b**_{DMA} (Fig. S15b-i), suggesting the formation of a bcc-type regular ordering structure of the MOP core even in the film form.

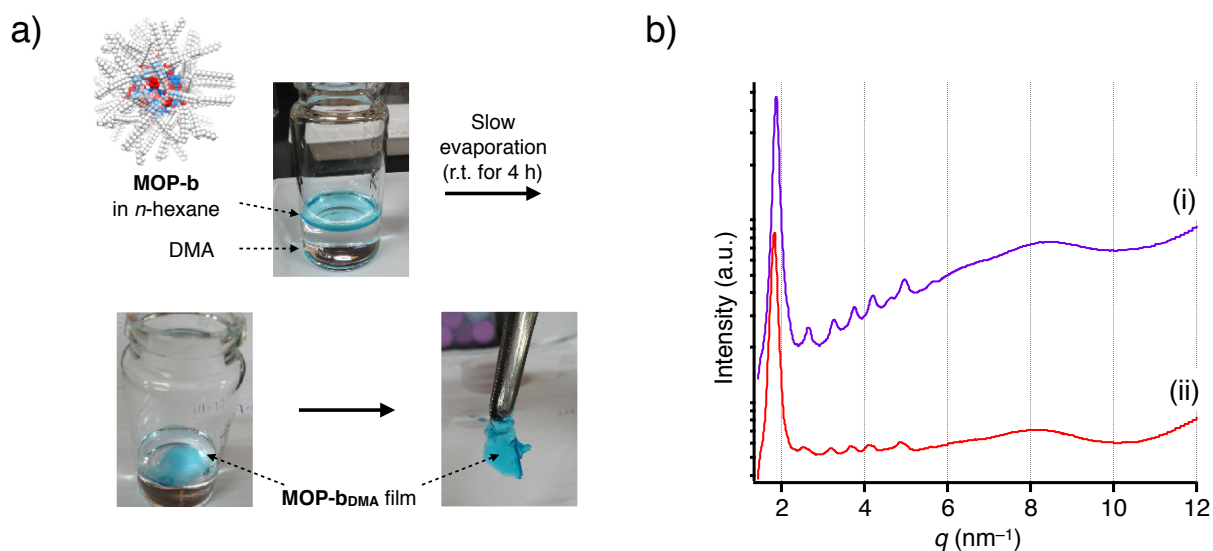


Figure S15. a) Preparation of liquid crystalline film of **MOP-b**_{DMA} via a solution-based process, b) XRD profiles of (i) **MOP-b**_{DMA} and (ii) **MOP-b**_{DMA} film (r.t., CuK α , $\lambda = 1.541$ Å).

6. Thermal analysis and discussion

Thermogravimetric analyses (TGA) were performed for dried **MOP-a** and **MOP-b**. The TGA profiles are shown in Figure S16. Both MOPs were stable up to 300 °C and significant weight losses corresponding to material decomposition were observed above ~320 °C.

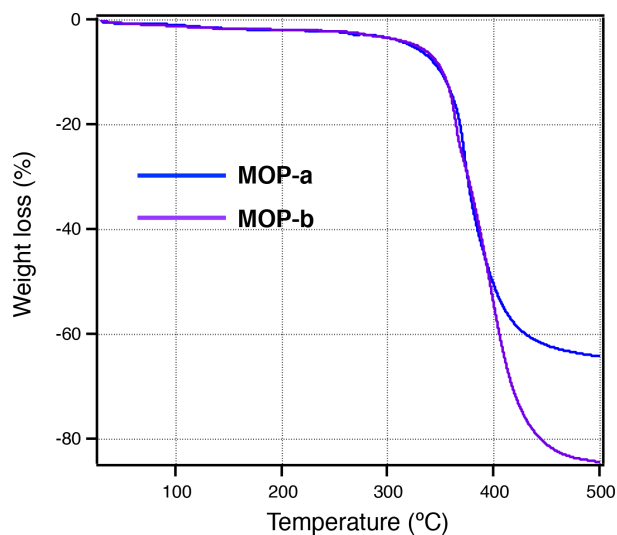


Figure S16. TGA profile of **MOP-a** and **MOP-b** under a N₂ flow (Heating rate: 5 °C/min)

The differential scanning calorimetry (DSC) profiles were measured for dried and DMA-impregnated MOPs, namely, **MOP-a**, **MOP-b**, **MOP-a_{DMA}**, and **MOP-b_{DMA}** at the heating rate of 10 °C/min under a N₂ flow. The DSC profiles are summarized in Figure S17.

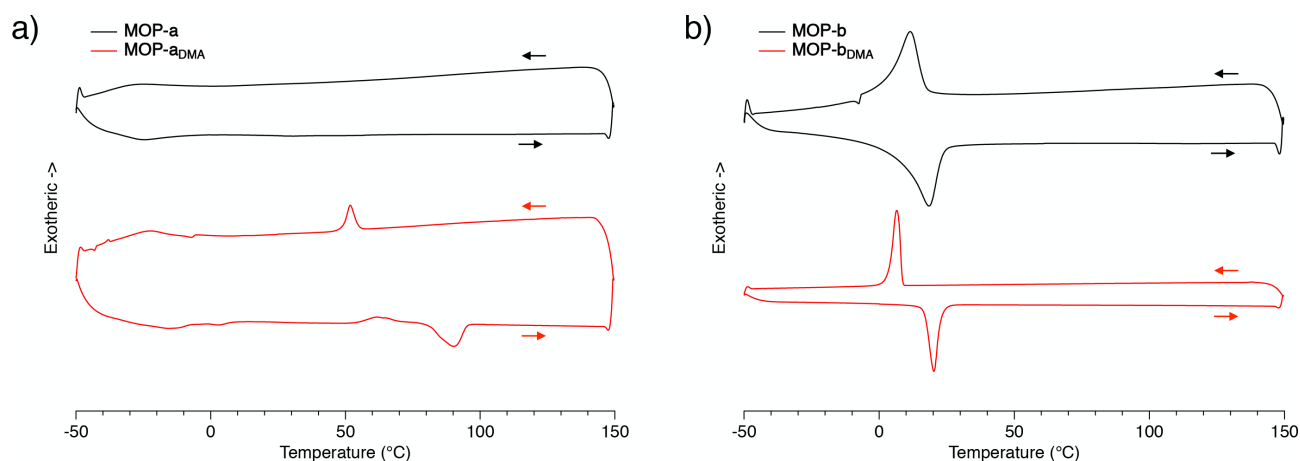


Figure S17. DSC profiles of a) **MOP-a** and **MOP-a_{DMA}**, and b) **MOP-b** and **MOP-b_{DMA}**.

In the DSC profile, DMA-impregnated MOP, **MOP-a_{DMA}**, showed exo/endothermic peaks at 50 °C upon cooling and 90 °C upon heating, respectively, which can be ascribed to LC phase transitions. On the other hand, **MOP-a** without DMA did not show any significant peak of phase transitions in the range of -50 to 150 °C (scan rate: 10 °C/min). The small broadened peaks around -25 °C can be due to the alkyl chain

crystallization. In contrast to **MOP-a**, both **MOP-b** and **MOP-b_{DMA}** showed peaks around 5-10 °C upon cooling and 15-20 °C upon heating, which may correspond to the alkyl chain crystallization.

Both **MOP-a** and **MOP-b** without DMA did not show melting behavior at high temperature until decomposition. Variable-temperature (SR) XRD profiles of as-synthesized **MOP-a** and **MOP-b** without DMA showed no difference in the random assembling structure and at given temperatures (Fig. S18) while the alkyl chain crystallization/solidification might take place at lower temperature below 5-10 °C in **MOP-b** (Fig. S17). It should be noted that the crystallization of **MOP-a** (Fig. S14) was observed only when **MOP-a_{DMA}** was slowly desiccated to be dried. This suggests that DMA plays an important role for the structuring of **MOP-a** into the three-dimensionally ordered phase.

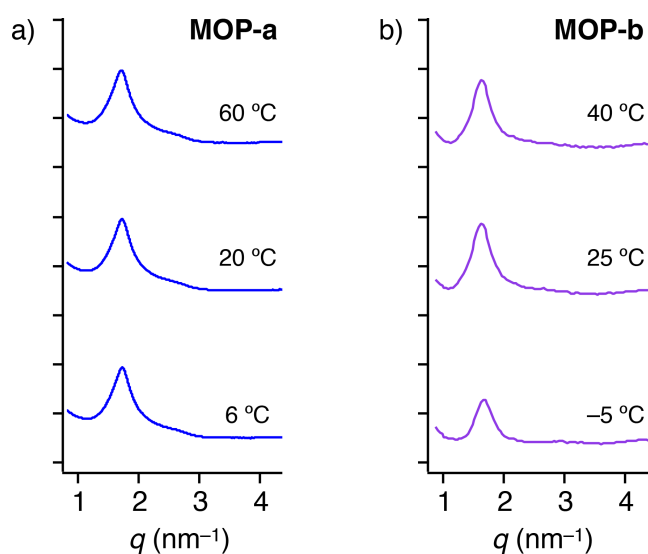


Figure S18. Variable-temperature (SR) XRD profiles of as-synthesized a) **MOP-a** and b) **MOP-b** without DMA. Those profiles of **MOP-a** and **MOP-b** were collected using synchrotron radiation X-ray beam of BL45XU ($\lambda = 1.0 \text{ \AA}$) at SPring-8, Japan and monochromatic X-ray ($\text{CuK}\alpha$) of Rigaku SmartLab diffractometer, respectively.

7. References

1. a) J. Wu, M. D. Watson, L. Zhang, Z. Wang and K. Müllen, *J. Am. Chem. Soc.*, 2004, **126**, 177–186; b) H. Maeda, Y. Haketa and T. Nakanishi, *J. Am. Chem. Soc.*, 2007, **129**, 13661–13674; c) C. Song, Y. Ling, Y. Feng, W. Zhou, T. Yildirim and Y. He, *Chem. Commun.*, 2015, **51**, 8508–8511.
2. a) J.-R. Li and H.-C. Zhou, *Nat. Chem.*, 2010, **2**, 893–898; b) N. Hosono, M. Gochomori, R. Matsuda, H. Sato and S. Kitagawa, *J. Am. Chem. Soc.*, 2016, **138**, 6525–6531.